106 *Biochemistry* **2011,** *50,* 106–115
DOI: 10.1021/bi101451g

BIOCHEMISTRY
including biophysical chemistry & molecular biology
Article

Characterization of the Estradiol-Binding Site Structure of Human Pancreas-Specific Protein Disulfide Isomerase: Indispensable Role of the Hydrogen Bond between His278 and the Estradiol 3-Hydroxyl Group[†]

Xin-Miao Fu, Pan Wang, and Bao Ting Zhu*

Department of Pharmacology, Toxicology and Therapeutics, School of Medicine, University of Kansas Medical Center, Kansas City, Kansas 66160, United States

Received September 8, 2010; Revised Manuscript Received November 10, 2010

ABSTRACT: Estradiol (E_2), a female sex hormone, has important biological functions. Human pancreas-specific protein disulfide isomerase (PDIp), a protein folding catalyst, was recently found to be able to bind E_2. Here we report the characterization of its E_2-binding site by using biochemical methods coupled with molecular modeling tools. Analysis of various truncated PDIp proteins showed that the $b-b'$ fragment contains an intact E_2-binding site that has the same binding affinity as the full-length PDIp protein, with apparent K_d values of approximately 170 nM. Computational modeling and docking analyses revealed that the E_2-binding site in the $b-b'$ fragment is located in a hydrophobic pocket composed mainly of the b' domain and partially of the b domain. The hydrogen bond, formed between the 3-hydroxyl group of E_2 (donor) and PDIp's His278 (acceptor), is indispensable for its binding. By contrast, the 17β-hydroxyl group of E_2 is of negligible importance for E_2 binding. This binding model was jointly confirmed by a series of experiments, such as selective mutation of the binding site amino acid residues and selective modification of the ligand structures.

Estradiol (E_2),[1] an important endogenous female sex hormone, exerts a wide array of biological functions in various target organs or tissues in a woman's body, such as the development of reproductive organs and secondary sex characteristics. Many of the well-known physiological functions of E_2 are mediated by the genomic actions of estrogen receptors α and β (*1*), which are transcription factors that can initiate the expression of various target genes. In addition, the nongenomic actions of ERs have also been suggested to play a role in mediating E_2-induced rapid signal transduction in certain systems (*2*, *3*).

Besides ERs, a few other proteins have also been found to have the ability to bind endogenous estrogens, serving as important modulators of the biological actions of these female hormones. For instance, the sex hormone binding globulin (SHBG), a well-known estrogen-binding protein present in large quantities in circulation, can profoundly modulate the bioavailability of free circulating estrogens, subsequently altering the tissue and intracellular levels of estrogens and their hormonal activity in various target sites (*4*, *5*). Protein disulfide isomerase (PDI), a well-known protein folding catalyst for disulfide bond formation (*6*, *7*), can also bind estrogens (*8*−*10*) and modulate the estrogen level and hormonal actions in human breast cancer cells (*11*). Recently, we reported, for the first time, that the human pancreas-specific PDI homologue (PDIp), which is strongly expressed in pancreatic acinar cells (*12*, *13*) and has both disulfide isomerase (*12*, *14*) and chaperone activities (*14*, *15*), is another intracellular E_2-binding protein that can modulate estrogen actions in mammalian cells (*16*). In light of these earlier observations, and also given the fact that these two intracellular proteins are present at unusually high levels in certain human tissues or cells [e.g., the pancreatic PDIp accounts for approximately 0.1% of the total cellular protein (*16*)], there was speculation that PDI and PDIp may function as important intracellular E_2 storage proteins in these cells (*9*, *11*, *16*). In addition, the recent observation showing the copresence of PDIp with ERα and ERβ in the pancreas of humans and animals (*16*) also points to the possibility that PDIp may be a viable modulator of the actions of endogenous estrogens in this nonclassical target tissue.

At present, the E_2-binding site structures of human PDI and PDIp are not known, although a few earlier studies have suggested that their peptide-binding sites may overlap with their E_2-binding sites (*9*, *15*, *17*). Elucidation of the estrogen-binding site structures of these intracellular proteins is of considerable interest because it will aid in the identification of potential xenobiotics that may be able to alter estrogen action by modulating the estrogen binding activity of these intracellular proteins. The main purpose of this study, therefore, was to delineate the structural basis of human PDIp's E_2 binding activity. Through a combined use of computational modeling analysis, site-directed mutagenesis, and selective ligand modifications, we located the PDIp's E_2-binding site to a hydrophobic pocket between the b' and b domains. In addition, we have also built the PDIp−E_2 binding model and have identified a hydrogen bond formed between His278 of PDIp and the 3-hydroxyl group of E_2 to be essential for their binding interaction.

MATERIALS AND METHODS

Chemicals, Reagents, Cell Lines, and Tissues. E_2 and its structural analogues were purchased from Steraloids (Newport, RI).

[†]This study was supported, in part, by a grant from the National Institutes of Health (CA97109).

*To whom correspondence should be addressed. Phone: (913) 588-9842. Fax: (913) 588-7501. E-mail: BTZhu@kumc.edu.

[1]Abbreviations: PDI, protein disulfide isomerase; PDIp, pancreas-specific PDI homologue; ERα and ERβ, estrogen receptors α and β, respectively; E_2, estradiol; SEC, size-exclusion chromatography; SDS−PAGE, sodium dodecyl sulfate−polyacrylamide gel electrophoresis.

 Published on Web 11/16/2010

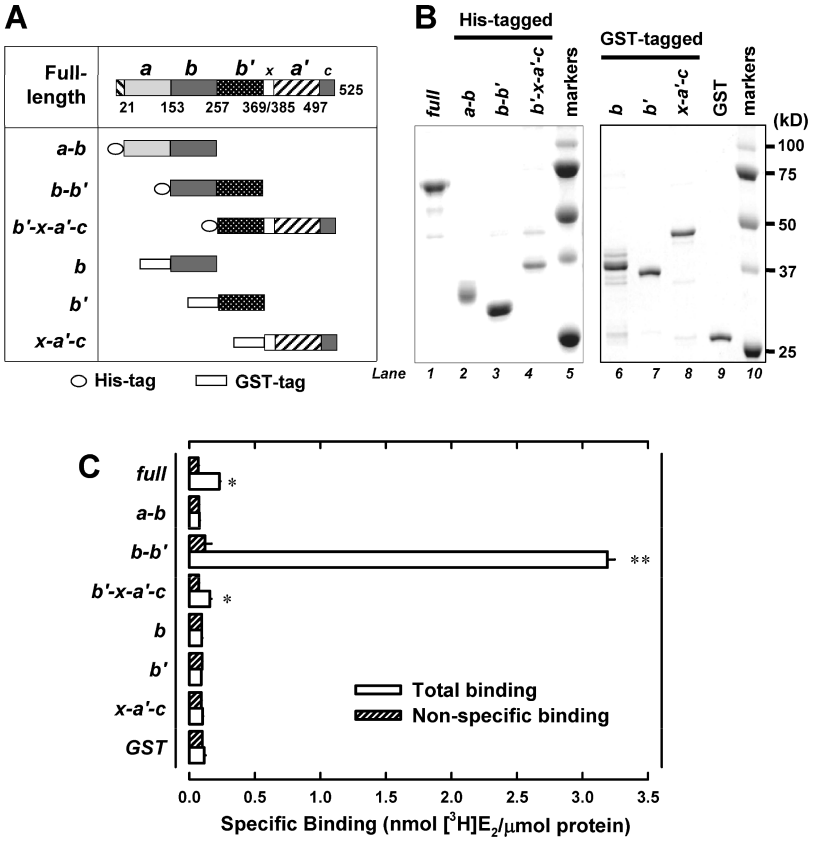

FIGURE 1: Human PDIp $b-b'$ fragment containing the E_2-binding site. (A) Domain organization of the human PDIp protein (based on UniProtKB entry Q13087). Domain boundaries of human PDIp are determined by sequence alignment of PDIp with PDI, whose domain boundaries were described previously (*28*). Fragments $a-b$, $b-b'$, and $b'-x-a'-c$ were constructed as histidine-tagged fusion proteins. The b, b', and $x-a'-c$ fragments were constructed as GST-tagged fusion proteins. (B) SDS−PAGE analysis of three histidine-tagged PDIp fragments (left part) and three GST-tagged fragments (right part), which were selectively expressed in *E. coli* cells and then purified using chromatography. (C) Binding of [^{3}H]E_2 by each of the purified PDIp fragments (at a final concentration of 0.5 μM) after incubation with 4.5 nM [^{3}H]E_2 in 10 mM sodium phosphate buffer (pH 7.4) in the absence or presence of 10 μM cold E_2. Each value is the mean ± standard deviation (SD) of triplicate determinations. Compared to the corresponding nonspecific binding, $^*P < 0.05$ and $^{**}P < 0.01$. In other experiments, P values were also < 0.05 (for the $b'-x-a'-c$ domain) or < 0.01 (for the $b-b'$ domain).

[^{3}H]E_2 (specific activity of 110 Ci/mmol) was obtained from Perkin-Elmer (Waltham, MA). Mastoparan (Ile-Asn-Leu-Lys-Ala-Leu-Ala-Ala-Leu-Ala-Lys-Lys-Ile-Leu) was obtained from Sigma-Aldrich (St. Louis, MO). All other chemicals and reagents used in this study were of analytical grade or higher. The mouse anti-PDIp antiserum (1:2500 dilution for Western blotting) was raised in our laboratory (*16*). The monkey kidney cos-7 cells were obtained from the ATCC (Manassas, VA) and cultured in the DMEM medium supplemented with 10% fetal bovine serum (FBS).

Plasmid Construction and Protein Purification. Human PDIp (its cDNA clone was obtained from ATCC, catalog no. 6706839) was cloned into the pET-19b vector at the sites of 5′-NdeI/XhoI-3′ without a signal peptide and also cloned into the pcDNA3.1 vector with a signal peptide at the sites of 5′-HindIII/XhoI-3′. The plasmids for the expression of histidine-tagged truncated PDIp proteins ($a-b$, $b-b'$, and $b'-x-a'-c$ fragments) were constructed by cloning the corresponding cDNA sequences into a modified pET-19b vector as described previously (*16*). Purification of the recombinant histidine-tagged proteins expressed in *Escherichia coli* was conducted as described previously (*14*, *16*). The PDIp b, b', and $x-a'-c$ fragments were cloned into a modified pGEX-4T-1 vector containing the NdeI sites at 5′-NdeI/SalI-3′ and expressed as the GST-tagged fusion proteins. After being expressed in *E. coli* cells, these proteins were purified using the Glutathione Sepharose 4 Fast Flow column (GE Healthcare). Site-directed mutagenesis was performed using the Phusion Site-Directed Mutagenesis Kit from New England Biolabs according to the manufacturer's instructions.

[^{3}H]E_2 Binding Assay for Purified PDIp Proteins. Desalting was employed to separate the free [^{3}H]E_2 and protein-bound [^{3}H]E_2 as described previously (*16*). Proteins were incubated with [^{3}H]E_2 (typically at a final concentration of 4.5 nM) in 10 mM sodium phosphate buffer (pH 7.4) at 4 °C overnight. The incubation mixture (100 μL) was subjected to desalting using the PD miniTrap G-25 columns (from GE health) pre-equilibrated with 10 mM sodium phosphate buffer (pH 7.4, 0.15 M NaCl). Eluted fractions from 0.5 to 1.15 mL were collected and mixed with 3 mL of the scintillation cocktail (Fisher Scientific, Pittsburgh, PA) for radioactivity measurement on a Beta Counter (Perkin-Elmer). For saturation experiments, increasing concentrations of [^{3}H]E_2 were present during the incubation. The nonspecific binding was assessed in the presence of excess nonradiolabeled E_2 (10 μM).

Computational Homology Modeling. Because the X-ray structure of the human PDIp $b-b'$ fragment is not available at present, the human PDI $b-b'$ domain structure [Protein Data Bank (PDB) entry 2k18] (*18*) was thus used as a template to build the homology structural model for the human PDIp $b-b'$ fragment. Protein sequence alignment shows that the sequence identity between the human PDIp $b-b'$ fragment and the human

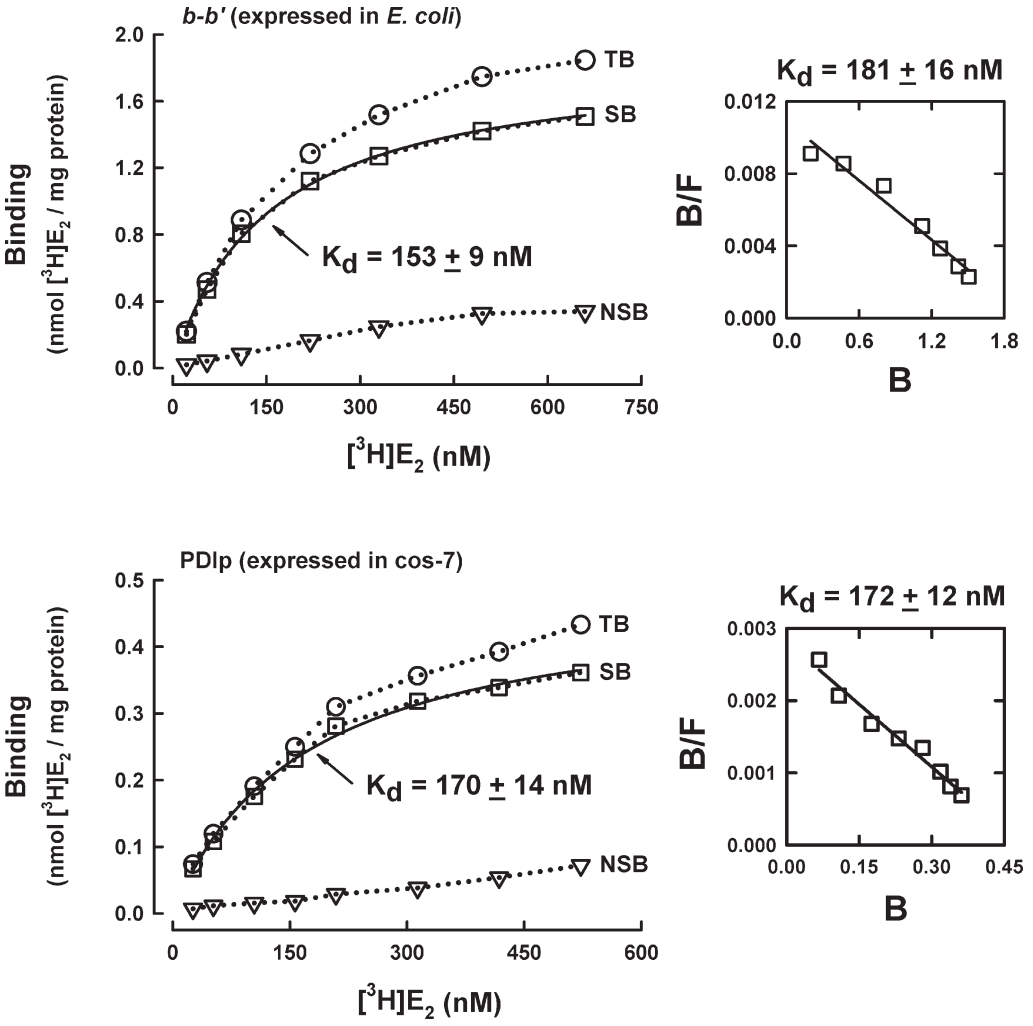

FIGURE 2: Determination of the dissociation constant (K_d) of the human $b-b'$ fragment and the full-length human PDIp for E_2. The total binding (TB) of [^{3}H]E_2 by the $b-b'$ fragment or the full-length PDIp protein (at a final concentration of 20 μg/mL) was determined in the presence of increasing concentrations of [^{3}H]E_2 (22−660 nM) in 10 mM sodium phosphate buffer (pH 7.4). The nonspecific binding (NSB) was determined in the presence of excess nonradiolabeled E_2 (10 μM). Total binding (TB) with NSB subtracted gives rise to specific binding (SB). The binding curve (left part) was obtained using curve regression analysis (hyperbola model) of SigmaPlot. The corresponding Scatchard plot is shown in the right part of each panel. Panel A shows the data obtained with the purified recombinant PDIp $b-b'$ fragment expressed in *E. coli* cells. Panel B shows the data for the purified human PDIp protein selectively expressed in cos-7 cells (the purification procedures are described in the Supporting Information and shown in Figure S1). Each value is the mean of duplicate measurements.

PDI $b-b'$ fragment is 38% (data presented in Results and Discussion). The *Homology Modeling* module of *Insight II* (Accelrys, Inc., San Diego, CA) was used to generate the three-dimensional structure model for the human PDIp $b-b'$ fragment. The side chain rotamers were manually optimized to minimize the intramolecular bump, and then the protein structure was further optimized with the *Discover* module of *Insight II*.

Binding Site Determination and Molecular Docking. The E_2-binding sites on the homology structural model of the human PDIp $b-b'$ fragment were identified by using the *Active-Site-Search* function in the *Binding-Site* module of *Insight II*. The *site-open-size* parameter was set at 5 Å, and the *site-cutoff-size* parameter was set at 150 Å^3. We defined the binding pocket with amino acid residues within 5 Å of the candidate binding site. The *Simulated Annealing* docking method in the *Affinity* module was used to dock E_2 into the candidate binding pocket. Water molecules were excluded, and side chains in the binding site were allowed to move in the docking analysis. One hundred docking modes were calculated, and the ones with the lowest binding energy were chosen for further minimization.

RESULTS AND DISCUSSION

As depicted in Figure 1A, the human PDIp protein is a large protein composed of four thioredoxin-like domains, *a*, *b*, *b′*, and *a′*, and a small linker region *x* between *b′* and *a′* and a C-terminal acidic extension *c*. To experimentally locate the E_2-binding site in this protein, we designed three truncated human PDIp fragments (namely, $a-b$, $b-b'$, and $b'-x-a'-c$, as depicted in Figure 1A), with a His tag attached to their N-termini for the convenience of purification. Because these three fragments cover the full length of the PDIp protein with each fragment containing two neighboring main domains (i.e., $a-b$, $b-b'$, and $b'-a'$), theoretically they would allow us to determine whether the E_2-binding site is only associated with any of the individual domains or jointly formed by any of the two neighboring domains. These three PDIp fragments as designed above were selectively overexpressed in *E. coli* cells and purified (left part of Figure 1B) and then subjected to in vitro analysis of their [^{3}H]E_2 binding ability. The results (Figure 1C) showed that the $b-b'$ fragment has a distinct, high specific binding activity for [^{3}H]E_2, although a weak binding activity was also detected for the $b'-x-a'-c$ fragment. No

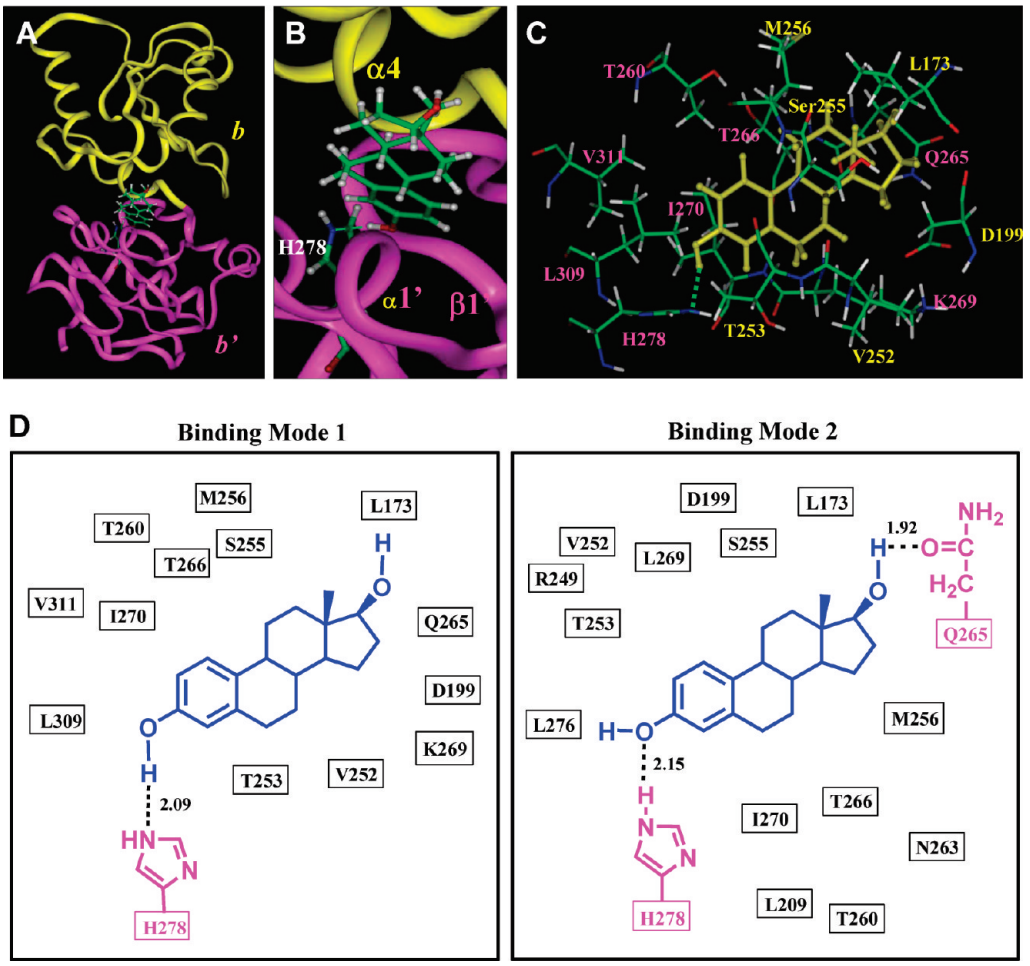

FIGURE 3: Docking analysis of the binding mode of E_2 inside the human PDIp $b-b'$ fragment. (A) Overview of the docking result (mode I) of E_2 binding inside the PDIp $b-b'$ fragment. E_2 and H278 are shown in the ball-and-stick format and colored according to atoms. The protein structure is shown as a ribbon. The yellow region represents the b domain and the magenta region the b' domain. (B) Close-up view of the docking result of the E_2−PDIp binding model, showing that a hydrogen bond is formed between the 3-hydroxyl group of E_2 (a hydrogen bond donor) and PDIp's His278 (a hydrogen bond acceptor). (C) Interaction of E_2 with amino acid residues in the binding pocket (mode I). Labeling of amino acid residues is shown in yellow for the b domain and in magenta for the b' domain. The E_2 molecule is colored yellow. Amino acids are shown in the ball-and-stick format and colored according to atoms, i.e., green for carbon, red for oxygen, white for hydrogen, and blue for nitrogen. (D) Plots of the docking results of E_2 binding with the PDIp $b-b'$ fragment in modes I and II. The distances are in angstroms. E_2 is colored blue, and H278 and Q265 are colored magenta.

binding activity was detected for the $a-b$ fragment when it was assayed at an equivalent molar protein concentration under the same conditions. These observations were repeated by using proteins prepared from over four independent experiments, and the $b-b'$ fragment was consistently found to have a very high E_2 binding activity. Accordingly, these results suggest that the E_2-binding site is not associated with each individual domain, but with the $b-b'$ domain complex.

To further verify the observations described above, next we selectively expressed the single b and b' domains for testing of their individual E_2 binding activity. In our initial experiments, we also adopted the strategy of attaching a His tag to the b and b' single-domain fragments. Unfortunately, the yield of the b and b' single-domain proteins (with a His tag) was very low when they were individually expressed in *E. coli* cells, likely because of their much smaller sizes and lower stabilities. After we modified the strategy by attaching a GST tag to the N-termini of the b and b' fragments, the problem of low protein yield was solved. The b and b' single-domain fragments (with a GST tag) were purified (Figure 1B) and then subjected to analysis of their ability to bind [^{3}H]E_2. However, the protein fragment that contained either the b or b' single domain did not have an appreciable [^{3}H]E_2 binding activity (Figure 1C). The experiment was repeated three times, and each time the same observations were made. For comparison, we have also prepared the single a' domain (in the form of $x-a'-c$), and this fragment also did not have appreciable [^{3}H]E_2 bidning activity (Figure 1C).

Using the purified $b-b'$ fragment, next we determined its E_2 binding affinity (i.e., the K_d value) when different concentrations (1−650 nM) of the radiolabeled E_2 were tested as the binding ligand. Analysis of the binding curve pattern as well as the Scatchard plot suggests that the PDIp $b-b'$ fragment displays single-binding site kinetics, with an apparent K_d value of 153−181 nM (Figure 2A). To verify that the human PDIp has only a single E_2-binding site, we also determined the [^{3}H]E_2 binding affinity of the full-length PDIp that was selectively overexpressed in the cos-7 mammalian cells. The preparation and purification of this protein are summarized in Figure S1 of the Supporting Information. Similarly, analysis of the binding curve pattern and Scatchard plot shows that the recombinant full-length human PDIp protein also exhibits single-site binding kinetics, with an apparent K_d value of approximately 170 nM

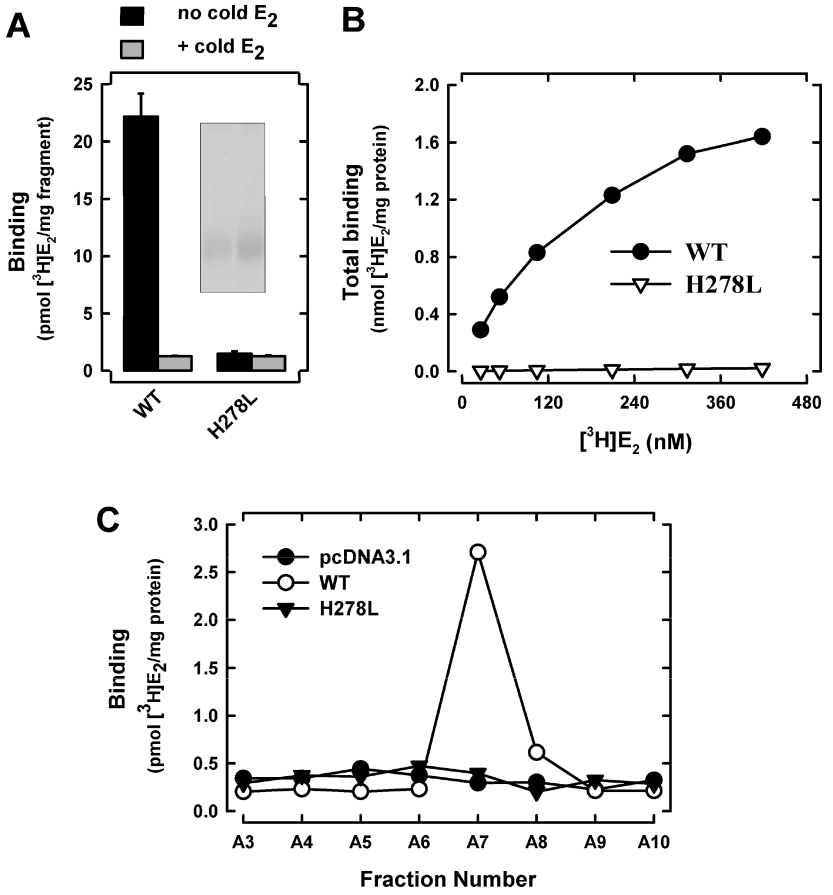

FIGURE 4: H278L mutant protein that lacks E_2 binding activity. (A) Total [^{3}H]E_2 binding by purified PDIp $b-b'$ fragments (wild-type and H278L mutant proteins, purified from *E. coli* cells) after incubation with 4.5 nM [^{3}H]E_2 in the absence or presence of excess cold E_2 (10 μM) in 10 mM sodium phosphate buffer. The inset shows the SDS−PAGE analysis of the purified proteins. (B) Total [^{3}H]E_2 binding by PDIp $b-b'$ fragments (at the final concentration of 20 μg/mL, wild-type protein and H278L mutant protein) determined in the presence of increasing concentrations of [^{3}H]E_2 (from 26 to 420 nM) in 10 mM sodium phosphate buffer (pH 7.4). (C) Total [^{3}H]E_2 binding by SEC fractions of cos-7 cell lysates containing the expressed full-length wild-type PDIp or the H278L mutant protein (see Figure S4 of the Supporting Information). The final concentration of [^{3}H]E_2 in these incubations was 4.5 nM. Each value is the mean of duplicate determinations.

(Figure 2B), which is very similar to the apparent K_d value of the purified recombinant $b-b'$ fragment. Notably, the K_d value of the full-length PDIp purified from *E. coli* cells was approximately 1500 nM (*16*), which is much higher than the K_d values for the $b-b'$ fragment purified from *E. coli* cells and the full-length PDIp purified from mammalian cells. We suspect that the lower E_2 binding affinity of the full-length PDIp expressed in *E. coli* cells might be due to impact folding of the protein. Taken together, these observations suggest that the human PDIp protein has only a single binding site for E_2, and the binding site is located in its $b-b'$ fragment.

Next we sought to predict the three-dimensional (3D) E_2-binding pocket structure of the PDIp $b-b'$ fragment by using computational modeling analysis. To achieve this goal, we first built the 3D structure of the $b-b'$ fragment by using the homology modeling approach according to the known structure of the $b-b'$ fragment of the human PDI protein (*18*), which is 38% identical in sequence with the human PDIp (as shown in Figure S2A of the Supporting Information). On the basis of the homology structural model of the human PDIp $b-b'$ fragment, we noticed that its backbone structure is very similar to that of the human PDI $b-b'$ fragment (Figure S2B of the Supporting Information). The most notable differences between these two structures are β5 and the starting region of α4, where PDIp has four more amino acid residues. The other small differences between these two structures are in the α3′ region, because of the difference in their amino acid compositions.

To predict the E_2-binding pocket in the $b-b'$ fragment, we used the *Insight II* modeling program to calculate the size of the cavities present in the protein structure. Three cavities were found in the $b-b'$ fragment (Figure S2C of the Supporting Information): cavity I located between the b and b' domains, i.e., formed jointly by these two domains (cavity size of 376 Å^3). In comparison, cavity II is solely formed by the b domain (size of 207 Å^3), and cavity III is solely formed by the b' domain (size of 129 Å^3). On the basis of the experimental data that showed that the single b or b' domain does not have an intact E_2-binding site whereas the $b-b'$ domain complex has the binding site, these experimental data were considered as the scientific basis for excluding cavities II and III for further consideration as viable E_2-binding sites. By contrast, cavity I matches the experimental findings; i.e., the binding pocket is formed by both b and b' domains but not by the individual domain present alone. Here it should also be noted that cavity I also has an optimal size that would enable it to function as a low-affinity E_2-binding site. Earlier studies (*19*−*21*) showed that the volumes of the E_2-binding pockets of human ERα and ERβ are 266 and 275 Å^3, respectively. The fact that cavity I (376 Å^3) is slightly larger than the E_2-binding pockets of human ERs suggests that E_2 likely will bind more loosely inside PDIp's binding pocket than inside the binding pockets of ERs, which agrees well with the

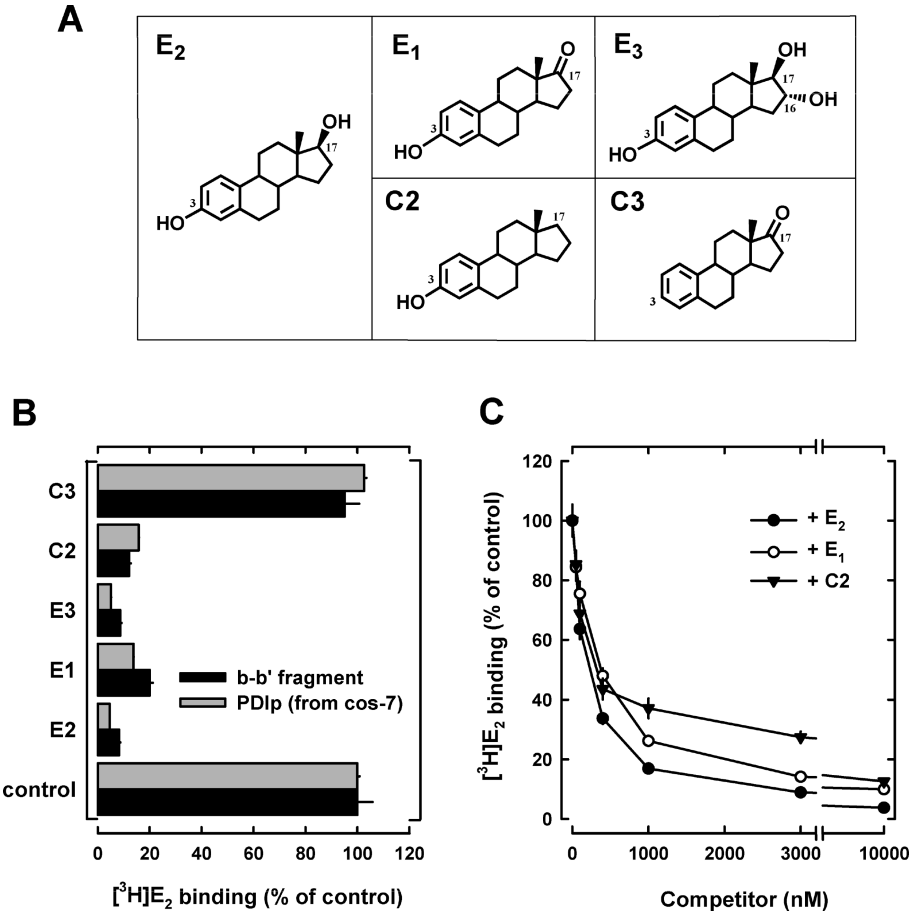

FIGURE 5: Relative binding activity of PDIp for several E_2 derivatives. (A) Chemical structures of E_2 and several of its analogues used in this study. (B) Relative binding of [^{3}H]E_2 by the recombinant PDIp $b-b'$ fragment (at a final concentration of 20 μg/mL, purified from *E. coli* cells) (see Figure 1B) or by purified recombinant full-length PDIp protein expressed in cos-7 cells [at a final concentration of 20 μg/mL (see Figure S1 of the Supporting Information)]. Protein was incubated with 4.5 nM [^{3}H]E_2 in the absence or presence of 10 μM E_2 or its analogues in sodium phosphate buffer (10 mM, pH 7.4). (C) Relative [^{3}H]E_2 binding by the PDIp $b-b'$ fragment purified from *E. coli* cells after incubation with 4.5 nM [^{3}H]E_2 in 10 mM sodium phosphate buffer (pH 7.4) in the absence (control, set as 100%) or presence of increasing concentrations of E_2, E_1, and C2. Each value is the mean ± SD of triplicate determinations.

known differences in their E_2 binding affinities. On the other hand, the much smaller sizes of cavities I and II compared to those of the human ERs further suggest that they are unlikely to be viable E_2-binding sites.

Next, we used the *Affinity* module of *Insight II* to dock E_2 into cavity I. The overall E_2−PDIp binding interaction is shown in panels A and B of Figure 3, and the amino acid residues surrounding the binding pocket are shown in Figure 3C. Two candidate E_2 binding modes are suggested (Figure 3D). In both binding modes, E_2 has a very similar overall orientation and positioning inside the binding pocket, and hydrogen bonds are formed between E_2 and the PDIp $b-b'$ fragment. In mode I (left part of Figure 3D), one hydrogen bond is formed between the 3-hydroxyl group of E_2 and the nitrogen atom of His278 of PDIp. In mode II (right part of Figure 3D), two hydrogen bonds are formed: one between the 3-hydroxyl group of E_2 and His278 of PDIp and the other between the 17-hydroxyl group of E_2 and Gln265 of PDIp. To experimentally test the binding modes as suggested by our computational docking analysis, we first sought to determine whether the two identified amino acid residues, His278 and Gln265, are indeed involved in the binding interactions between PDIp and E_2 through the formation of hydrogen bonds. To do so, we introduced point mutations to probe whether changes in these two amino acid residues would alter PDIp's E_2 binding activity.

We first chose to mutate His278 to leucine (H278L). According to earlier studies (*22*, *23*), the side chain length of leucine is similar to that of histidine, but the leucine does not contain electronegative atoms that are necessary for the formation of hydrogen bonds. As shown in Figure 4A, the purified H278L $b-b'$ fragment completely lost its [^{3}H]E_2 binding activity. A saturation binding assay further confirmed that this mutant fragment did not have appreciable [^{3}H]E_2 binding activity even when very high concentrations of [^{3}H]E_2 were present (Figure 4B). Similarly, we also introduced the H278L mutation into full-length PDIp, which was overexpressed in mammalian cells and isolated by SEC (Figure S3 of the Supporting Information). An assay of the [^{3}H]E_2 binding activity of each of the SEC fractions showed that the PDIp H278L mutant protein does not have appreciable [^{3}H]E_2 binding activity (Figure 4C). Taken together, these data show that PDIp's His278 is indispensable for its binding interaction with E_2.

Using the same approach, we also mutated Gln265 to leucine (Q265L). As suggested by binding mode II (Figure 3D), Gln265 may form a hydrogen bond with the 17-hydroxyl group of E_2. [^{3}H]E_2 binding assays showed that the purified Q265L $b-b'$ fragment [overexpressed in *E. coli* cells (Figure S4A of the Supporting Information)] and the full-length PDIp Q265L mutant protein [overexpressed in cos-7 cells (Figure S4B of the Supporting Information)] each display [^{3}H]E_2 binding activity

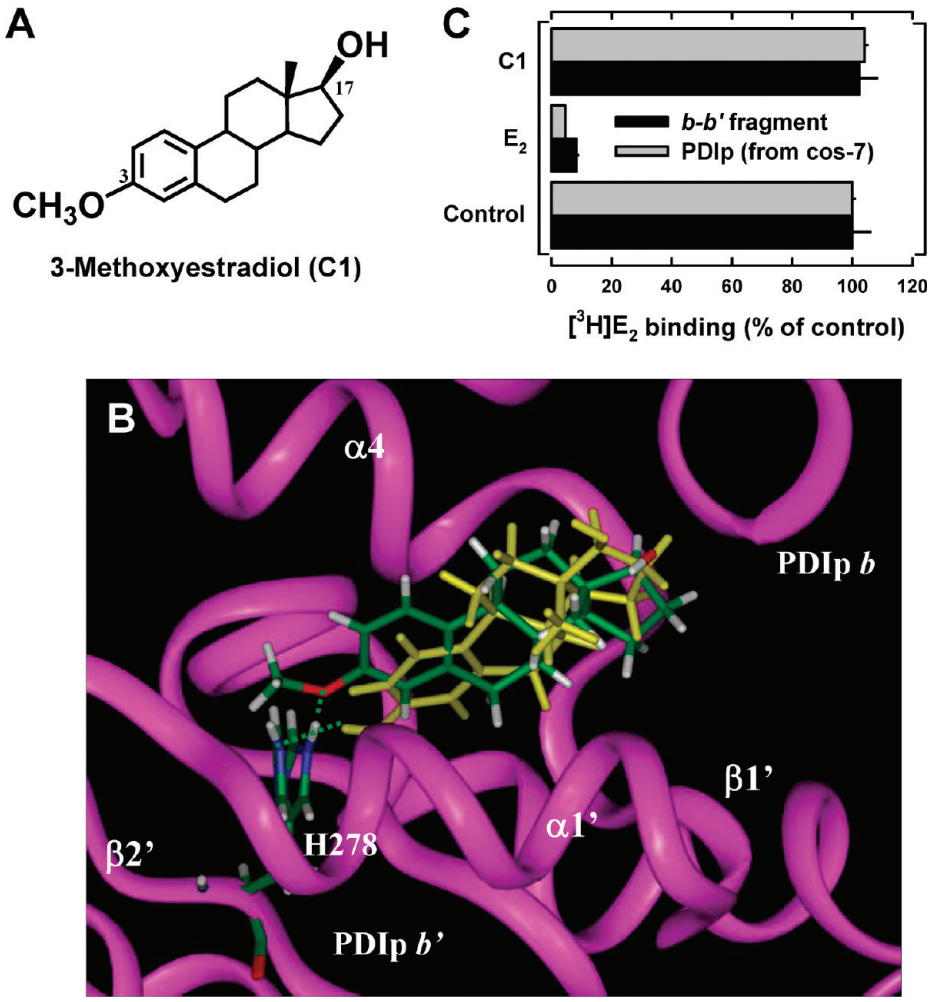

FIGURE 6: Docking analysis of the interaction of PDIp with E_2 analogue C1. (A) Chemical structure of 3-methoxyestradiol (C1). (B) Docking analysis of the modes of binding of E_2 and C1 in the binding pocket of the PDIp $b-b'$ fragment. The protein structure is shown as a ribbon and colored magenta. E_2, C1, and His278 are shown in the ball-and-stick format. C1 and His278 are colored according to atoms, and E_2 is colored yellow. Green dashes denote hydrogen bonds. α-Helices and β-sheets are labeled according to Figure S2A of the Supporting Information. (C) Relative [^{3}H]E_2 binding by the recombinant PDIp $b-b'$ fragment or by purified recombinant full-length PDIp in the absence or presence of 10 μM E_2 or its C1 analogue. Each value is the mean ± SD of triplicate determinations.

similar to that of the corresponding wild-type proteins. The apparent K_d value for Q265L $b-b'$ fragment was found to be 185 ± 8 nM (Figure S4C of the Supporting Information), which is nearly the same as that of the wild-type $b-b'$ fragment. In addition, we have also prepared the double mutant protein Q265L/H278L for testing its [^{3}H]E_2 binding activity. As expected, this double mutant protein does not have any [^{3}H]E_2 binding activity. Collectively, these observations suggest that PDIp's Gln265 either may form a nonessential, weak hydrogen bond with the 17-hydroxyl group of E_2 [as suggested by binding mode II (Figure 3D)] or may not form a viable hydrogen bond at all [as suggested by binding mode I (Figure 3D)]. In addition, we performed the in silico analysis (using *Insight II*) to predict the effect of point mutations (H278L and Q265L) on the structures of the PDIp $b-b'$ fragment. No appreciable differences were observed between the wild-type fragment and these two mutant fragments in terms of their secondary structures (which were also predicted by Jpred 3, http://www.compbio.dundee.ac.uk/www-jpred/) or tertiary structures (data not shown).

To provide further experimental support for the conclusions of the mutagenesis studies, we employed an alternative approach by using a number of E_2 derivatives that share the same core structure as E_2 but with their C-3 or C-17 hydroxyl group selectively modified such that they cannot form the same type of hydrogen bonds with PDIp that E_2 does. In these experiments, both the purified $b-b'$ fragment (expressed in *E. coli* cells) and purified full-length recombinant human PDIp (expressed in cos-7 cells) were used to assay their relative binding activity by measuring their ability to compete off the binding of [^{3}H]E_2. We found that E_1, E_3, and C2, all of which contain an intact 3-hydroxyl group but differ in their 17-hydroxyl group (structures shown in Figure 5A), could efficiently compete with [^{3}H]E_2 for binding to the $b-b'$ fragment or full-length PDIp (Figure 5B). There is no significant difference among the IC_{50} values of E_2, E_1, and C2 (Figure 5C). In contrast, C3, which lacks the 3-hydroxyl group (Figure 5A), displayed no appreciable binding activity (Figure 5B). These observations provide further support for the suggestion that the 3-hydroxyl group of E_2 is essential for the binding interaction with PDIp via the formation of hydrogen bond(s), whereas the 17-hydroxyl group of E_2 is not important. These results are in agreement with the observations made with the point mutation studies as described above.

Notably, while the two binding modes suggested by the docking studies are very similar in their overall structure and binding interaction, there are also some notable subtle differences. In mode I (Figure 3D), the 3-hydroxyl group of E_2 is a

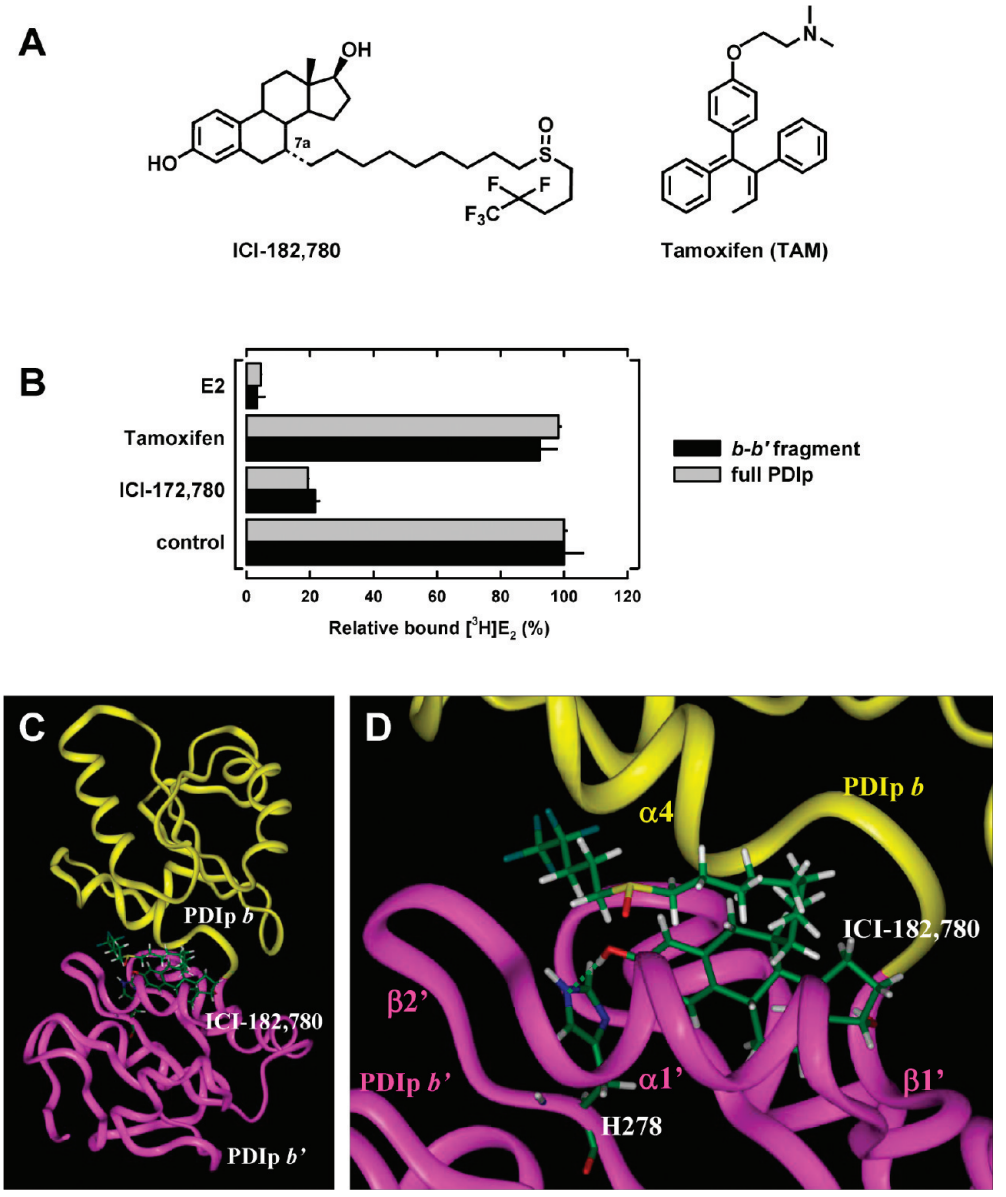

FIGURE 7: Docking analysis of the interaction of PDIp with ICI-172,780. (A) Chemical structures of ICI-172,780 and tamoxifen. (B) Relative [^{3}H]E_2 binding in the absence or presence of excess E_2, tamoxifen, or ICI compound (10 μM) by the recombinant PDIp $b-b'$ fragment (at a final concentration of 20 μg/mL, purified from *E. coli* cells) or by the recombinant full-length PDIp protein (at a final concentration of 20 μg/mL, purified from cos-7 cells). These proteins were incubated with 4.5 nM [^{3}H]E_2 in sodium phosphate buffer (10 mM, pH 7.4). Each data point is the mean ± SD of triplicate determinations. (C) Docking results showing the binding interaction of ICI-172,780 with the PDIp $b-b'$ fragment. (D) Close-up view of the docking result of ICI-172,780 binding in the PDIp $b-b'$ fragment, showing that a hydrogen bond (represented by the green dashed line) was formed between the 3-hydroxyl group of ICI-172,780 (hydrogen bond donor) and His278 of PDIp (hydrogen bond acceptor). The protein structure is shown as a ribbon. Yellow regions represent the b domain and magenta regions the b' domain. ICI-172,780 and His278 are shown in ball-and-stick format and colored according to atoms. α-Helices and β-sheets are labeled according to Figure S2A of the Supporting Information.

hydrogen bond donor and the nitrogen atom of His278 of PDIp is a hydrogen bond acceptor. In mode II, the 3-hydroxyl group of E_2 serves as a hydrogen bond acceptor and His278 of PDIp as a hydrogen bond donor in the formation of a hydrogen bond. On the basis of our earlier experience, it is almost certain that only one of the modes is the preferred binding mode. On the basis of the known difference in the strength of the OH−N hydrogen bond (6.9 kcal/mol) versus the O−HN hydrogen bond (1.9 kcal/mol) (*24*), it is predicted that binding mode I, which contains the stronger OH−N hydrogen bond, would be the preferred binding mode over mode II, which contains the weaker O−HN hydrogen bond. To provide experimental evidence for this prediction, we chose to determine the binding activity of 3-methoxyestradiol (structure shown in Figure 6A) for PDIp. Theoretically, the oxygen atom in the 3-methoxy group of 3-methoxyestradiol will be able to serve only as a hydrogen bond acceptor, not as a hydrogen bond donor, in forming a hydrogen bond (i.e., it can bind to PDIp only in mode I, not in mode II). Computational docking analysis showed that 3-methoxyestradiol can still bind inside the pocket in a similar way like E_2, because there is enough space around His278 to fully accommodate the methoxy group (Figure 6B). As expected, the computational binding model showed that 3-methoxyestradiol (serving as a hydrogen bond acceptor) still can form a hydrogen bond with His278 (serving as a hydrogen bond donor). However, in the binding assay, we found that 3-methoxyestradiol has no appreciable binding

activity for the $b-b'$ fragment or full-length PDIp (Figure 6C). This experimental observation suggests that the hydrogen bond formed between 3-methoxyestradiol and His278 likely is extremely weak or, more likely, not formed at all. Taking all the data together, we conclude that E_2 binds to PDIp by forming a hydrogen bond between the 3-hydroxyl group of E_2 and His278 of PDIp according to mode I, but not mode II (Figure 3D).

The results of this study also provide a good explanation for our early observation that while PDIp has no appreciable binding affinity for tamoxifen, it still retains considerable binding affinity for ICI-172,780 (*16*) (also see Figure 7B). It is known that tamoxifen does not have a phenolic OH group in its structure (see Figure 7A) and thus cannot form the necessary hydrogen bond with His278 of PDIp. In comparison, ICI-172,780 has the same core steroid structure as E_2 (see Figure 7D). Our docking analysis showed that ICI-172,780 can still be bound inside PDIp's binding pocket in a manner like that of E_2 (Figure 7C,D), although its long side chain at the C-7 position slightly interferes with the binding, which is consistent with its lower binding affinity (Figure 7B).

On the basis of the sequence and structural similarities between their $b-b'$ fragments (Figure S2A,B of the Supporting Information), it is suggested that PDI and PDIp may share a similar overall E_2-binding pocket, although additional experimental evidence is needed to verify this possibility. Despite their potential structural similarity, it is of interest to note that the affinity of PDI for E_2 [~1500 nM, as reported previously (*9*, *10*)] is considerably lower than that of PDIp. The lower binding affinity of PDI for E_2 was also reflected in another study that showed that the peptide binding activity of PDI is markedly less sensitive to the competitive inhibition by E_2 compared to the peptide binding activity of PDIp (*15*).

Notably, it is well-known that the 3-hydroxyl group of E_2 plays an essential role in its binding interaction with human ERα and ERβ by forming hydrogen bonds (*19*, *25*, *26*). The structural model developed in this study offers a good explanation for the experimental observation that the human PDIp has a much lower E_2 binding affinity than human ERs, for the following reasons. (i) PDIp forms only one hydrogen bond with the 3-hydroxyl group of E_2, whereas human ERs form two hydrogen bonds with this hydroxyl group. (ii) Whereas the 17β-hydroxyl group of E_2 plays an important role in its interaction with human ERα or ERβ (*25*), its role in the interaction with human PDIp appears to be of minimal importance or simply nonexistent. (iii) The E_2-binding site of PDIp is significantly larger than those of human ERα and ERβ; i.e., it is less compact, which would suggest a relatively looser binding interaction. (iv) For both ERα and ERβ, almost all amino acid residues in their binding pockets, except those that form hydrogen bonds with E_2, are hydrophobic residues, which provide stronger hydrophobic interactions with the four aliphatic rings of E_2. However, in the case of PDIp, some polar residues (Thr253, Thr260, Thr266, Ser225, and Gln265 shown in Figure 3C,D) are also present in the binding pocket, which may weaken the hydrophobic interactions with E_2. These notable differences distinguish human ERs from PDIp in their binding interactions with E_2.

Lastly, it is of note that observations made in this study may also shed light on understanding the binding interaction of PDIp with its substrate peptides, which was shown to be inhibited by E_2 and its analogues (*15*, *17*). In support of this suggestion, we found that mastoparan, a peptide that can bind to PDIp and the binding of which can be inhibited by E_2 as reported in an early study (*15*), can inhibit PDIp's [^{3}H]E_2 binding activity (Figure S5 of the Supporting Information). Therefore, the reciprocal inhibition of PDIp's ligand binding activity between E_2 and mastoparan suggests that they share the same or partially overlapping binding site in PDIp. Interestingly, an earlier study reported that the specificity of the peptide substrates during their interaction with PDIp is associated with the tyrosine and/or tryptophan residues in the peptide substrates (*27*). Because these two residues contain a free phenolic hydroxyl group and phenolic amine group, respectively, it is tempting to suggest that these amino acid residues may serve as hydrogen bond donors in forming hydrogen bonds with His278 of PDIp during PDIp−peptide interaction, in a manner similar to that observed for the 3-hydroxyl phenolic group in E_2. This possibility merits further investigation.

In conclusion, the human PDIp has a single E_2-binding site (apparent K_d of approximately 170 nM), and its E_2-binding site is located in a hydrophobic pocket largely composed of the b' domain and partially of the b domain. The hydrogen bond formed between the 3-hydroxyl group of E_2 (hydrogen bond donor) and His278 of PDIp (hydrogen bond acceptor) is indispensable for E_2 binding.

ACKNOWLEDGMENT

We thank Dr. Grace Liejun Guo in our department for recommending that we use the gel filtration system in her laboratory for the purification of the recombinant PDIp. Some of the instruments employed in this study are part of the COBRE core facility that is supported by National Institutes of Health Grant P20RR021940 from the National Center for Research Resources.

SUPPORTING INFORMATION AVAILABLE

Isolation of the wild-type and H278L PDIp proteins (Figures S1 and S3, respectively), homology modeling results for the $b-b'$ fragment (Figure S2), and E_2 binding activity of the Q265L mutant protein and inhibitory effect of a peptide on E_2 binding (Figures S4 and S5, respectively). This material is available free of charge via the Internet at http://pubs.acs.org.

REFERENCES

1. Ciocca, D. R., and Roig, L. M. (1995) Estrogen receptors in human nontarget tissues: Biological and clinical implications. *Endocr. Rev. 16*, 35–62.
2. Razandi, M., Pedram, A., Merchenthaler, I., Greene, G. L., and Levin, E. R. (2004) Plasma membrane estrogen receptors exist and functions as dimers. *Mol. Endocrinol. 18*, 2854–2865.
3. Li, L., Haynes, M. P., and Bender, J. R. (2003) Plasma membrane localization and function of the estrogen receptor α variant (ER46) in human endothelial cells. *Proc. Natl. Acad. Sci. U.S.A. 100*, 4807–4812.
4. Fortunati, N., and Catalano, M. G. (2006) Sex hormone-binding globulin (SHBG) and estradiol cross-talk in breast cancer cells. *Horm. Metab. Res. 38*, 236–240.
5. Zhang, Y., Graubard, B. I., Klebanoff, M. A., Ronckers, C., Stanczyk, F. Z., Longnecker, M. P., and McGlynn, K. A. (2005) Maternal hormone levels among populations at high and low risk of testicular germ cell cancer. *Br. J. Cancer 92*, 1787–1793.
6. Hatahet, F., and Ruddock, L. W. (2009) Protein disulfide isomerase: A critical evaluation of its function in disulfide bond formation. *Antioxid. Redox Signaling 11*, 2807–2850.
7. Wilkinson, B., and Gilbert, H. F. (2004) Protein disulfide isomerase. *Biochim. Biophys. Acta 1699*, 35–44.
8. Tsibris, J. C., Hunt, L. T., Ballejo, G., Barker, W. C., Toney, L. J., and Spellacy, W. N. (1989) Selective inhibition of protein disulfide isomerase by estrogens. *J. Biol. Chem. 264*, 13967–13970.
9. Primm, T. P., and Gilbert, H. F. (2001) Hormone binding by protein disulfide isomerase, a high capacity hormone reservoir of the endoplasmic reticulum. *J. Biol. Chem. 276*, 281–286.

10. Hiroi, T., Okada, K., Imaoka, S., Osada, M., and Funae, Y. (2006) Bisphenol A binds to protein disulfide isomerase and inhibits its enzymatic and hormone-binding activities. *Endocrinology 147*, 2773–2780.
11. Fu, X., Wang, P., and Zhu, B. T. (2008) Protein disulfide isomerase is a multifunctional regulator of estrogenic status in target cells. *J. Steroid Biochem. Mol. Biol. 112*, 127–137.
12. Desilva, M. G., Lu, J., Donadel, G., Modi, W. S., Xie, H., Notkins, A. L., and Lan, M. S. (1996) Characterization and chromosomal localization of a new protein disulfide isomerase, PDIp, highly expressed in human pancreas. *DNA Cell Biol. 15*, 9–16.
13. Desilva, M. G., Notkins, A. L., and Lan, M. S. (1997) Molecular characterization of a pancreas-specific protein disulfide isomerase, PDIp. *DNA Cell Biol. 16*, 269–274.
14. Fu, X. M., and Zhu, B. T. (2010) Human pancreas-specific protein disulfide-isomerase (PDIp) can function as a chaperone independently of its enzymatic activity by forming stable complexes with denatured substrate proteins. *Biochem. J. 429*, 157–169.
15. Klappa, P., Stromer, T., Zimmermann, R., Ruddock, L. W., and Freedman, R. B. (1998) A pancreas-specific glycosylated protein disulphide-isomerase binds to misfolded proteins and peptides with an interaction inhibited by oestrogens. *Eur. J. Biochem. 254*, 63–69.
16. Fu, X., and Zhu, B. T. (2009) Human pancreas-specific protein disulfide isomerase homolog (PDIp) is an intracellular estrogen-binding protein that modulates estrogen levels and actions in target cells. *J. Steroid Biochem. Mol. Biol. 115*, 20–29.
17. Klappa, P., Freedman, R. B., Langenbuch, M., Lan, M. S., Robinson, G. K., and Ruddock, L. W. (2001) The pancreas-specific protein disulphide-isomerase PDIp interacts with a hydroxyaryl group in ligands. *Biochem. J. 354*, 553–559.
18. Denisov, A. Y., Maattanen, P., Dabrowski, C., Kozlov, G., Thomas, D. Y., and Gehring, K. (2009) Solution structure of the bb′ domains of human protein disulfide isomerase. *FEBS J. 276*, 1440–1449.
19. Brzozowski, A. M., Pike, A. C., Dauter, Z., Hubbard, R. E., Bonn, T., Engstrom, O., Ohman, L., Greene, G. L., Gustafsson, J. A., and Carlquist, M. (1997) Molecular basis of agonism and antagonism in the oestrogen receptor. *Nature 389*, 753–758.
20. Manas, E. S., Unwalla, R. J., Xu, Z. B., Malamas, M. S., Miller, C. P., Harris, H. A., Hsiao, C., Akopian, T., Hum, W. T., Malakian, K., Wolfrom, S., Bapat, A., Bhat, R. A., Stahl, M. L., Somers, W. S., and Alvarez, J. C. (2004) Structure-based design of estrogen receptor-β selective ligands. *J. Am. Chem. Soc. 126*, 15106–15119.
21. Manas, E. S., Xu, Z. B., Unwalla, R. J., and Somers, W. S. (2004) Understanding the selectivity of genistein for human estrogen receptor-β using X-ray crystallography and computational methods. *Structure 12*, 2197–2207.
22. Birukou, I., Schweers, R. L., and Olson, J. S. (2010) Distal histidine stabilizes bound O_2 and acts as a gate for ligand entry in both subunits of adult human hemoglobin. *J. Biol. Chem. 285*, 8840–8854.
23. Yoshiro, M., Jun, F., Susumu, K., Kenji, O., Yuji, S., Yasuo, H., and Kazuyuki, M. (1997) Site-Directed Mutagenesis of His-176 and Glu-177 in *Pseudomonas aeruginosa* Alkaline Protease: Effect on Catalytic Activity. *J. Ferment. Bioeng. 84*, 588–590.
24. Emsley, J. (1980) Very Strong Hydrogen Bonds. *Chem. Soc. Rev. 9*, 91–124.
25. Zhu, B. T., Han, G. Z., Shim, J. Y., Wen, Y., and Jiang, X. R. (2006) Quantitative structure-activity relationship of various endogenous estrogen metabolites for human estrogen receptor α and β subtypes: Insights into the structural determinants favoring a differential subtype binding. *Endocrinology 147*, 4132–4150.
26. Gabbard, R. B., and Segaloff, A. (1983) Structure-activity relationships of estrogens. Effects of 14-dehydrogenation and axial methyl groups at C-7, C-9 and C-11. *Steroids 41*, 791–805.
27. Ruddock, L. W., Freedman, R. B., and Klappa, P. (2000) Specificity in substrate binding by protein folding catalysts: Tyrosine and tryptophan residues are the recognition motifs for the binding of peptides to the pancreas-specific protein disulfide isomerase PDIp. *Protein Sci. 9*, 758–764.
28. Tian, G., Xiang, S., Noiva, R., Lennarz, W. J., and Schindelin, H. (2006) The crystal structure of yeast protein disulfide isomerase suggests cooperativity between its active sites. *Cell 124*, 61–73.